

E. Muljadi
C. P. Butterfield

National Renewable Energy Laboratory,
Golden, Colorado 80401

H. Romanowitz
Oak Creek Energy Systems Inc.,
Mojave, California 93501

R. Yinger
Southern California Edison,
Rosemead, California 91770

Self-Excitation and Harmonics in Wind Power Generation

Traditional wind turbines are commonly equipped with induction generators because they are inexpensive, rugged, and require very little maintenance. Unfortunately, induction generators require reactive power from the grid to operate; capacitor compensation is often used. Because the level of required reactive power varies with the output power, the capacitor compensation must be adjusted as the output power varies. The interactions among the wind turbine, the power network, and the capacitor compensation are important aspects of wind generation that may result in self-excitation and higher harmonic content in the output current. This paper examines the factors that control these phenomena and gives some guidelines on how they can be controlled or eliminated.

[DOI: 10.1115/1.2047590]

1 Introduction

Many of today's operating wind turbines have fixed speed induction generators that are very reliable, rugged, and low cost. During normal operation, an induction machine requires reactive power from the grid at all times. Thus, the general practice is to compensate reactive power locally at the wind turbine and at the point of common coupling where the wind farm interfaces with the outside world. The most commonly used reactive power compensation is capacitor compensation. It is static, low cost, and readily available in different sizes. Different sizes of capacitors are generally needed for different levels of generation. A bank of parallel capacitors is switched in and out to adjust the level of compensation. With proper compensation, the power factor of the wind turbine can be improved significantly, thus improving overall efficiency and voltage regulation. On the other hand, insufficient reactive power compensation can lead to voltage collapse and instability of the power system, especially in a weak grid environment.

Although reactive power compensation can be beneficial to the overall operation of wind turbines, we should be sure the compensation is the proper size and provides proper control. Two important aspects of capacitor compensation, self-excitation [1,2] and harmonics [3,4], are the subjects of this paper.

In Sec. 2, we describe the power system network; in Sec. 3, we discuss the self-excitation in a fixed-speed wind turbine; and in Sec. 4, we discuss harmonics. Finally, our conclusions are presented in Sec. 5.

2 Power System Network Description

We investigate a very simple power system network consisting of one 1.5 MW, fixed-speed wind turbine with an induction generator connected to a line feeder via a transformer (2 MVA, 3 phase, 60 Hz, 690 V/12 kV). The low-speed shaft operates at 22.5 rpm, and the generator rotor speed is 1200 rpm at its synchronous speed.

A diagram representing this system is shown in Fig. 1. The power system components analyzed include the following:

- An infinite bus and a long line connecting the wind turbine to the substation
- A transformer at the pad mount

- Capacitors connected in the low voltage side of the transformer
- An induction generator

For the self-excitation, we focus on the turbine and the capacitor compensation only (the right half of Fig. 1). For harmonic analysis, we consider the entire network shown in Fig. 1.

3 Self-Excitation

3.1 The Nature of Self-Excitation in an Induction Generator. Self-excitation is a result of the interactions among the induction generator, capacitor compensation, electrical load, and magnetic saturation. This section investigates the self-excitation process in an off-grid induction generator; knowing the limits and the boundaries of self-excitation operation will help us to either utilize or to avoid self-excitation.

Fixed capacitors are the most commonly used method of reactive power compensation in a fixed-speed wind turbine. An induction generator alone cannot generate its own reactive power; it requires reactive power from the grid to operate normally, and the grid dictates the voltage and frequency of the induction generator.

Although self-excitation does not occur during normal grid-connected operation, it can occur during off-grid operation. For example, if a wind turbine operating in normal mode becomes disconnected from the power line due to a sudden fault or disturbance in the line feeder, the capacitors connected to the induction generator will provide reactive power compensation, and the turbine can enter self-excitation operation. The voltage and frequency during off-grid operation are determined by the balance between the system's reactive and real power.

One potential problem arising from self-excitation is the safety aspect. Because the generator is still generating voltage, it may compromise the safety of the personnel inspecting or repairing the line or generator. Another potential problem is that the generator's operating voltage and frequency may vary. Thus, if sensitive equipment is connected to the generator during self-excitation, that equipment may be damaged by over/under voltage and over/under frequency operation. In spite of the disadvantages of operating the induction generator in self-excitation, some people use this mode for dynamic braking to help control the rotor speed during an emergency such as a grid loss condition. With the proper choice of capacitance and resistor load (to dump the energy from the wind turbine), self-excitation can be used to maintain the wind turbine at a safe operating speed during grid loss and mechanical brake malfunctions.

The equations governing the system can be simplified by looking at the impedance or admittance of the induction machine. To

Contributed by the Solar Energy Division of THE AMERICAN SOCIETY OF MECHANICAL ENGINEERS for publication in the ASME JOURNAL OF SOLAR ENERGY ENGINEERING. Manuscript received: February 28, 2005; revised received: July 22, 2005. Associate Editor: Dale Berg.

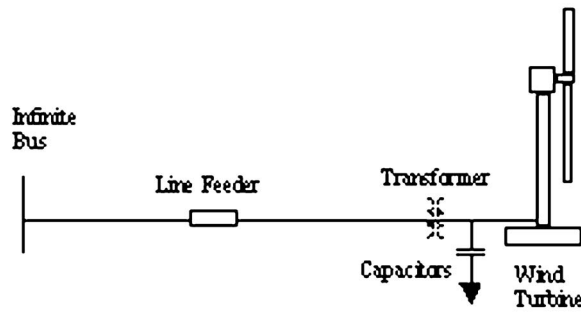


Fig. 1 The physical diagram of the system under investigation

operate in an isolated fashion, the total admittance of the induction machine and the rest of the connected load must be zero. The voltage of the system is determined by the flux and frequency of the system. Thus, it is easier to start the analysis from a node at one end of the magnetizing branch. Note that the term “impedance” in this paper is the conventional impedance divided by the frequency. The term “admittance” in this paper corresponds to the actual admittance multiplied by the frequency.

3.2 Steady-State Representation. The steady-state analysis is important to understand the conditions required to sustain or to diminish self-excitation. As explained above, self-excitation can be a good thing or a bad thing, depending on how we encounter the situation. Figure 2 shows an equivalent circuit of a capacitor-compensated induction generator. As mentioned above, self-excitation operation requires that the balance of both real and reactive power must be maintained. Equation (1) gives the total admittance of the system shown in Fig. 2:

$$Y_S + Y'_M + Y'_R = 0, \quad (1)$$

where

- Y_S = effective admittance representing the stator winding, the capacitor, and the load seen by node M
- Y'_M = effective admittance representing the magnetizing branch as seen by node M , referred to the stator side
- Y'_R = effective admittance representing the rotor winding as seen by node M , referred to the stator side

(Note: the superscript “ ’ ” indicates that the values are referred to the stator side.)

Equation (1) can be expanded into the equations for imaginary and real parts as shown in Eqs. (2) and (3):

$$\frac{R_{1L}/\omega}{(R_{1L}/\omega)^2 + L_{1L}^2} + \frac{R'_R/S\omega}{(R'_R/S\omega)^2 + L_{LR}^2} = 0 \quad (2)$$

where

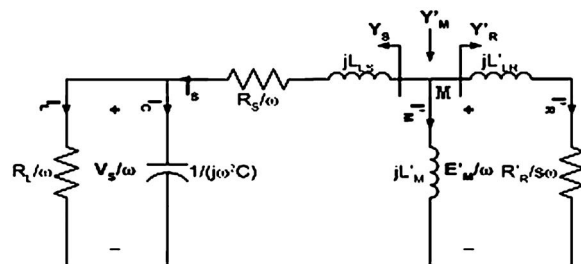


Fig. 2 Per phase equivalent circuit of an induction generator under self-excitation mode

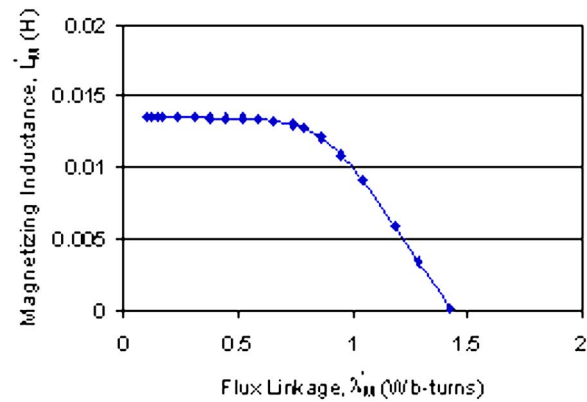


Fig. 3 A typical magnetization characteristic

$$\frac{1}{L'_M} + \frac{L_{1L}}{(R_{1L}/\omega)^2 + L_{1L}^2} + \frac{L'_{LR}}{(R'_R/S\omega)^2 + L_{LR}^2} = 0 \quad (3)$$

$$R_{1L} = R_S + \frac{R_L}{(\omega CR_L)^2 + 1}$$

$$L_{1L} = L_{LS} - \frac{CR_L}{(\omega CR_L)^2 + 1}$$

- R_S = stator winding resistance
- L_{LS} = stator winding leakage inductance
- R'_R = rotor winding resistance
- L'_{LR} = rotor winding leakage inductance
- L'_M = stator winding resistance
- S = operating slip
- ω = operating frequency
- R_L = load resistance connected to the terminals
- C = capacitor compensation

R_{1L} and L_{1L} are the effective resistance and inductance, respectively, representing the stator winding and the load as seen by node M .

One important aspect of self-excitation is the magnetizing characteristic of the induction generator. Figure 3 shows the relationship between the flux linkage and the magnetizing inductance for a typical generator; an increase in the flux linkage beyond a certain level reduces the effective magnetizing inductance L'_M . This graph can be derived from the experimentally determined no-load characteristic of the induction generator.

To solve the above equations, we can fix the capacitor (C) and the resistive load (R_L) values and then find the operating points for different frequencies. From Eq. (2), we can find the operating slip at a particular frequency. Then, from Eq. (3), we can find the corresponding magnetizing inductance L'_M , and, from Fig. 3, the operating flux linkage at this frequency. The process is repeated for different frequencies.

As a base line, we consider a capacitor with a capacitance of 3.8 mF (milli-farad) connected to the generator to produce approximately rated VAR (volt ampere reactive) compensation for full load generation (high wind). A load resistance of $R_L = 1.0 \Omega$ is used as the base line load. The slip versus rotor speed presented in Fig. 4 shows that the slip is roughly constant throughout the speed range for a constant load resistance. The capacitance does not affect the operating slip for a constant load resistance, but a higher resistance (R_L high=lower generated power) corresponds to a lower slip.

The voltage at the terminals of the induction generator (presented in Fig. 5) shows the impact of changes in the capacitance

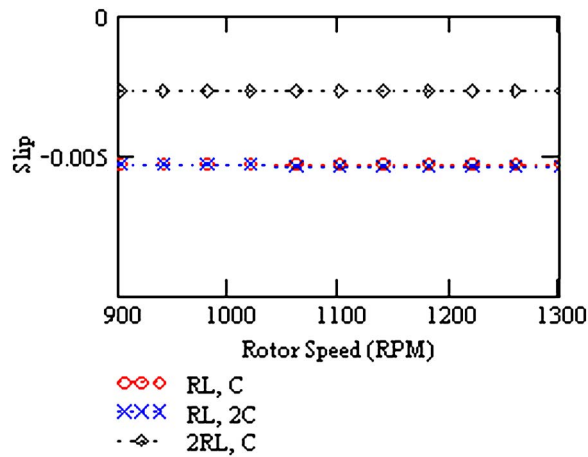


Fig. 4 Variation of slip for a typical self-excited induction generator

and load resistance. As shown in Fig. 5, the load resistance does not affect the terminal voltage, especially at the higher rpm (higher frequency), but the capacitance has a significant impact on the voltage profile at the generator terminals. A larger capacitance yields less voltage variation with rotor speed, while a smaller capacitance yields more voltage variation with rotor speed. As shown in Fig. 6, for a given capacitance, changing the effective value of the load resistance can modulate the torque-speed characteristic.

These concepts of self-excitation can be exploited to provide dynamic braking for a wind turbine (as mentioned above) to prevent the turbine from running away when it loses its connection to the grid; one simply needs to choose the correct values for capacitance (a high value) and load resistance to match the turbine power output. Appropriate operation over a range of wind speeds can be achieved by incorporating a variable resistance and adjusting it depending on wind speed.

3.3 Dynamic Behavior. This section examines the transient behavior in self-excitation operation. We choose a value of 3.8 mF capacitance and a load resistance of 1.0 Ω for this simulation. The constant driving torque is set to be 4500 Nm. Note that the wind turbine aerodynamic characteristic and the turbine control system are not included in this simulation because we are more interested in the self-excitation process itself. Thus, we fo-

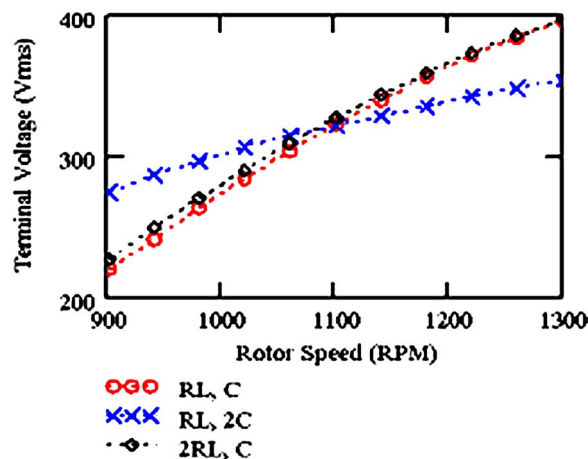


Fig. 5 Terminal voltage versus rotor speed for different R_L and C

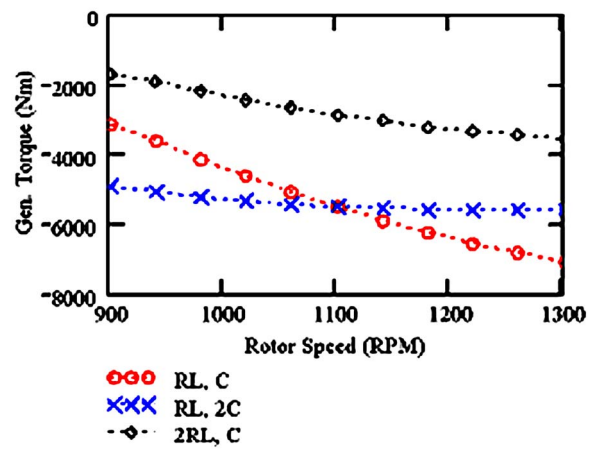


Fig. 6 The generator torque vs. rotor speed for different R_L and C

cus on the electrical side of the equations.

Figure 7 shows time series of the rotor speed and the electrical output power. In this case, the induction generator starts from rest. The speed increases until it reaches its rated speed. It is initially connected to the grid and at $t=3.1$ seconds (s), the grid is disconnected and the induction generator enters self-excitation mode. At $t=6.375$ s, the generator is reconnected to the grid, terminating the self-excitation. The rotor speed increases slightly during self-excitation, but, eventually, the generator torque matches the driving torque (4500 Nm), and the rotor speed is stabilized. When the generator is reconnected to the grid without synchronization, there is a sudden brief transient in the torque as the generator resynchronizes with the grid. Once this occurs, the rotor speed settles at the same speed as before the grid disconnection.

Figure 8(a) plots per phase stator voltage. It shows that the stator voltage is originally the same as the voltage of the grid to which it is connected. During the self-excitation mode ($3.1 \text{ s} < t < 6.375 \text{ s}$), when the rotor speed increases as shown in Fig. 7, the voltage increases and the frequency is a bit higher than 60 Hz. The voltage and the frequency then return to the rated values when the induction generator is reconnected to the grid. Figure 8(b) is an expansion of Fig. 8(a) between $t=3.0 \text{ s}$ and $t=3.5 \text{ s}$ to better illustrate the change in the voltage that occurs during that transient.

4 Harmonic Analysis

4.1 Simplified Per Phase Higher Harmonics Representation. In order to model the harmonic behavior of the network, we replace the power network shown in Fig. 1 with the per phase equivalent circuit shown in Fig. 9(a). In this circuit representation, a higher harmonic or multiple of 60 Hz is denoted

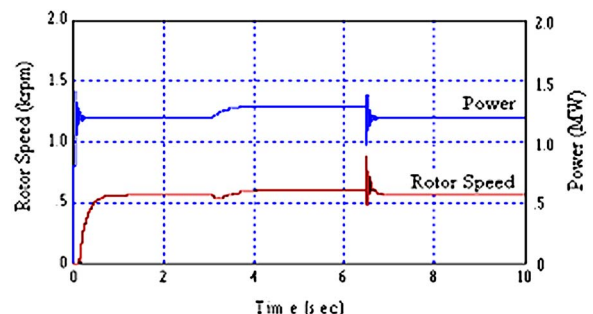


Fig. 7 The generator output power and rotor speed vs. time

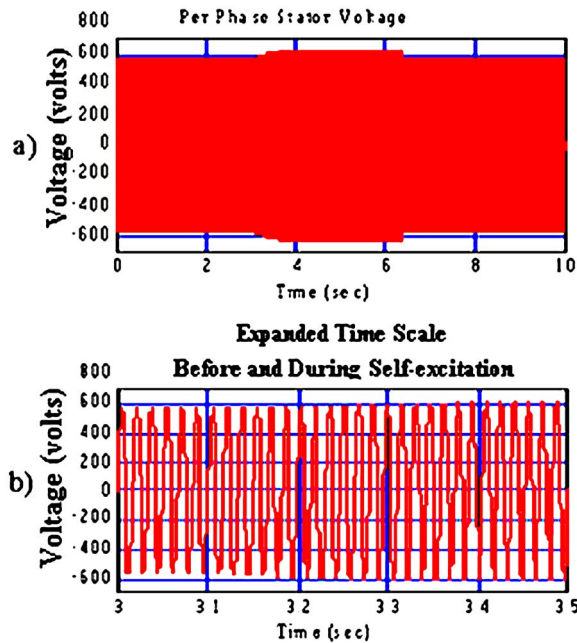


Fig. 8 The terminal voltage versus the time. (a) Voltage during self-excitation. (b) Voltage before and during self-excitation, and after reconnection.

by h , where h is the integer multiple of 60 Hz. Thus $h=5$ indicates the fifth harmonic (300 Hz). For wind turbine applications, the induction generator, transformer, and capacitors are three phase and connected in either Wye or Delta configuration, so the even harmonics and the third harmonic do not exist [5,6]. That is, only $h=5, 7, 11, 13, 17, \dots$, etc. exist.

4.1.1 Infinite Bus and Line Feeder. The infinite bus and the line feeder connecting the wind turbine to the substation are represented by a simple Thevenin representation of the larger power system network. Thus, we consider a simple RL line representation.

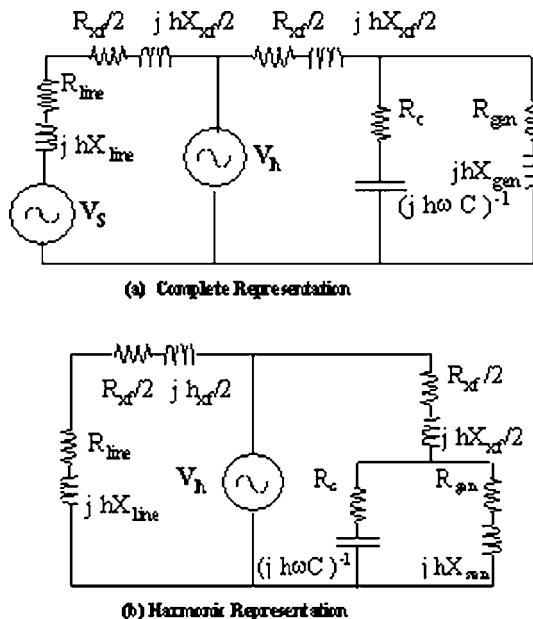


Fig. 9 The per phase equivalent circuit of the simplified model for harmonic analysis

4.1.2 Transformer. We consider a three-phase transformer with leakage reactance (X_{xf}) of 6 percent. Because the magnetizing reactance of a large transformer is usually very large compared to the leakage reactance ($X'_M \approx \infty \rightarrow$ open circuit), only the leakage reactance is considered. Assuming the efficiency of the transformer is about 98 percent at full load, and the copper loss is equal to the core loss (a general assumption for an efficient, large transformer), the copper loss and core loss are each approximately 1 percent or 0.01 per unit. With this assumption, we can compute the copper loss in per unit at full load current ($I_{1 \text{ Full Load}} = 1.0$ per unit), and we can determine the total winding resistance of the primary and secondary winding (about one percent in per unit).

4.1.3 Capacitor Compensation. Switched capacitors represent the compensation of the wind turbine. The wind turbine we consider is equipped with an additional 1.9 MVAR reactive power compensation (1.5 MVAR above the 400 kVAR supplied by the manufacturer). The wind turbine is compensated at different levels of compensation depending on the level of generation. The capacitor is represented by the capacitance C in series with the parasitic resistance (R_c), representing the losses in the capacitor. This resistance is usually very small for a good quality capacitor.

4.1.4 Induction Generator. The induction generator (1.5 MW, 480 V, 60 Hz) used for this wind turbine can be represented as the per phase equivalent circuit shown Fig. 9(a). The slip of an induction generator at any harmonic frequency h can be modeled as

$$S_h = \frac{h\omega_s - \omega_r}{h\omega_s} \quad (4)$$

where

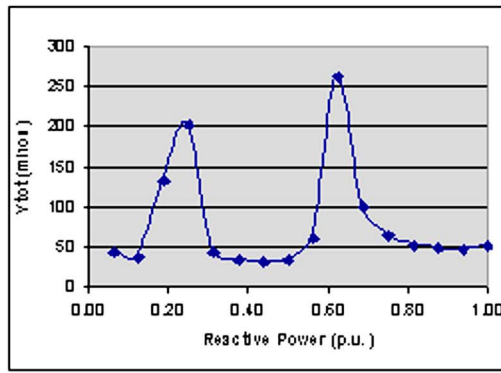
- S_h = slip for h th harmonic
- h = harmonic order
- ω_s = synchronous speed of the generator
- ω_r = rotor speed of the generator

Thus for higher harmonics (fifth and higher) the slip is close to 1 ($S_h=1$) and for practical purposes is assumed to be 1.

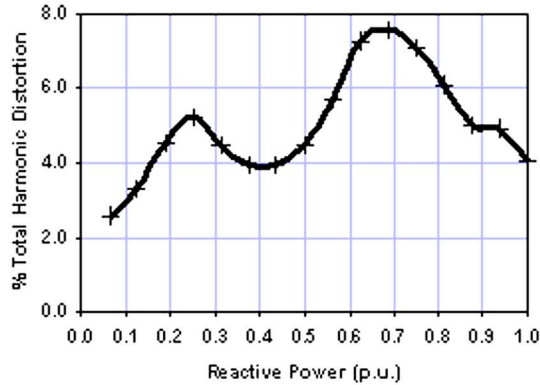
4.2 Steady State Analysis. Figure 9(b) shows the simplified equivalent circuit of the interconnected system representing higher harmonics. Note that the magnetizing inductance of the transformers and the induction generator are assumed to be much larger than the leakages and are not included for high harmonic calculations. In this section, we describe the characteristics of the equivalent circuit shown in Fig. 9, examine the impact of varying the capacitor size on the harmonic admittance, and use the result of calculations to explain why harmonic contents of the line current change as the capacitance is varied.

From the superposition theorem, we can analyze a circuit with only one source at a time while the other sources are turned off. For harmonics analysis, the fundamental frequency voltage source can be turned off. In this case, the fundamental frequency voltage source (infinite bus), V_s , is short circuited.

Wind farm operator experience shows us that harmonics occur when the transformer operates in the saturation region, that is, at higher flux levels as shown in Fig. 3. During the operation in this saturation region, the resulting current can be distorted into a sharply peaked sinusoidal current due to the larger magnetizing current imbedded in the primary current. This nonsinusoidal current can excite the network at resonant frequencies of the network. From the circuit diagram we can compute the impedance (at any capacitance and harmonic frequency) seen by the harmonic source, V_h , with Eq. (5), where the sign “||” represents the words “in parallel with:”



(a)



(b)

Fig. 10 (a) The total admittance for higher harmonics (odd and non-triplen) as a function of reactive compensation. (b) Total harmonic distortion of the current as a function of the reactive compensation in per unit.

$$Z(C, h) = (Z_{line} + 0.5Z_{xf}) \parallel (0.5Z_{xf} + Z_C \parallel Z_{gen}) \quad (5)$$

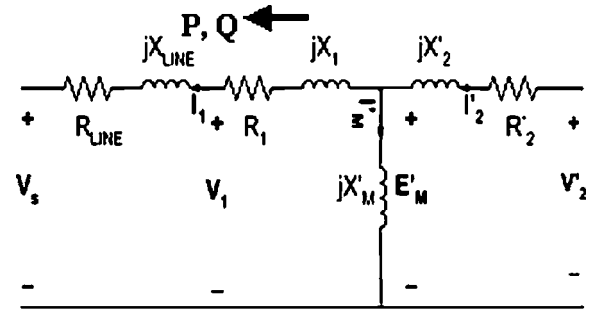
where

$$\begin{aligned} Z_{line} &= R_{line} + jX_{line} &&= \text{line impedance} \\ Z_{xf} &= R_{xf} + jX_{xf} &&= \text{transformer leakage impedance} \\ Z_C &= R_C + (jh\omega C)^{-1} &&= \text{capacitor impedance} \\ Z_{gen} &= R_{gen} + jX_{gen} &&= \text{generator impedance} \end{aligned}$$

The admittance at any capacitance and harmonic frequency can be found from the impedance:

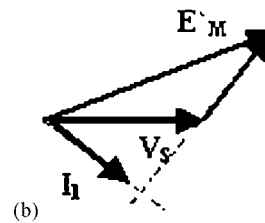
$$Y(C, h) = \frac{1}{Z(C, h)} \quad (6)$$

For a given harmonic, the harmonic current is proportional to the admittance shown in Eq. (6) multiplied by the corresponding harmonic voltage. Because the field data only consist of the total harmonic distortion of the capacitor current, and do not provide information about individual harmonics, we can only compare the trends from the admittance calculation to the measured data. Figure 10(a) shows the total calculated admittance for all harmonics of interest up to the 23rd harmonic excluding, as explained earlier, the even harmonics and all multiples of the third harmonic, plotted as a function of the total reactive power (in per unit). Changes in the reactive power are created by changing the size of the compensation capacitors. For comparison, the measured data of the total harmonic distortion as a function of the total reactive



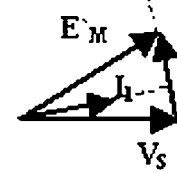
(a)

$P > 0, Q > 0$



(b)

$P > 0, Q < 0$



(c)

Fig. 11 (a) Per-phase equivalent circuit of a transformer. (b) Phasor diagram for $P > 0, Q > 0$. (c) Phasor diagram for $P > 0, Q < 0$.

power (in per unit) are presented in Fig. 10(b). Note that the two plots show very similar behavior—both exhibit resonance at reactive power levels around 0.25 and 0.65.

From Fig. 10, we can say that the circuit will resonate at different frequencies as the capacitor C is varied. Two harmonic components must exist to generate harmonics currents in the systems—a harmonic source (due to magnetic saturation as shown in Fig. 3) and a circuit that will resonate at certain levels of capacitance compensation.

4.3 Dynamic Simulation. Now consider how the harmonic sources are generated in the transformer. Most utility-size wind turbines are equipped with a pad-mount step-up transformer that connects them to the utility. When the transformer is saturated, the nonlinear characteristic of the magnetic circuit generates a non-sinusoidal current.

Figure 11(a) shows the per-phase equivalent circuit of a transformer. The iron core loss of a transformer is usually represented as an equivalent resistance, R'_{CORE} , in parallel with the magnetizing reactance X'_M . In this study, the core loss is small enough to be neglected (i.e., the value of $R'_{CORE} = \infty$ represents an open circuit; thus, the equivalent resistance R'_{CORE} is not drawn in the equivalent circuit). The magnetizing flux linkage is proportional to the ratio of the voltage and the frequency:

$$\lambda'_M \approx \frac{E'_M}{\omega_B} \quad (7)$$

where

$$\begin{aligned} E'_M &= \text{the magnetizing voltage} \\ \lambda'_M &= \text{flux linkage} \\ \omega_B &= \text{the base frequency} \end{aligned}$$

The flux linkage of the transformer can be found from Eq. (7). The relationship between the flux linkage and the magnetizing inductance L'_M due to the magnetizing current is nonlinear. When the magnetizing current is low, the flux (and flux linkage) varies linearly with the magnetizing current, but eventually saturation is

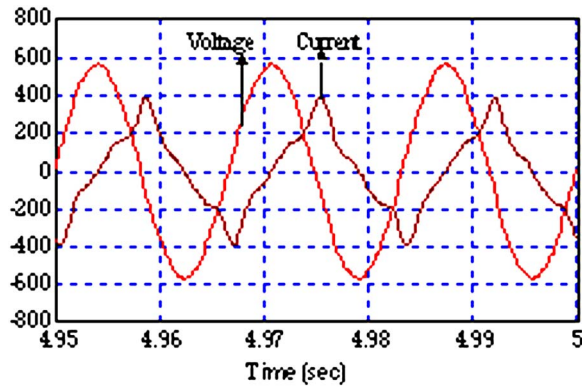


Fig. 12 The output voltage and current of a transformer under light load condition

reached and the nonlinear characteristic starts; further increases in magnetizing current I'_M will produce smaller increases in the flux linkage. In the saturation region, the resulting output current I'_2 will be nonsinusoidal, as shown in Fig. 12, due to the nonlinearity of the magnetizing inductance.

Additional details on the complete dynamic model for the three-phase transformer (including nonlinear magnetic saturation) may be found in [3]. We implemented this model in the simulation software discussed in [7].

There are two types of operation that can cause saturation. The first one occurs when the transformer operates at a higher voltage level; i.e., the voltage across E'_M is high. One example of this operation is when the transformer is lightly loaded; thus the voltage drop along the line feeder impedance ($R_{LINE} + jX_{LINE}$) and the voltage drop across the primary-winding impedance ($R_1 + jX_1$) are small. As a result, the magnetizing branch is exposed to a high voltage E'_M , producing a large magnetizing current I'_M in the magnetizing branch.

The second type of operation that can result in high saturation is when the transformer is operated with a leading power factor (supplying reactive power to the grid V_s).

The voltage across the magnetizing reactance X'_M (referred to the primary side) can be expressed as

$$E'_M = V_s + I_1(Z_{LINE} + Z_1) \quad (8)$$

where

Z_{LINE}	$= R_{LINE} + jX_{LINE}$	= line impedance connecting the transformer to the voltage source V_s
Z_1	$= R_1 + jX_1$	= primary winding impedance of the transformer
R_1	$= R'_2 = R_{xf}/2$	= resistance of the primary and secondary winding of the transformer
X_1	$= X'_2 = X_{xf}/2$	= leakage reactance of the primary and secondary winding of the transformer
V_s		= voltage at the infinite bus
I_1		= current flowing in the primary winding
X_{LINE}		= reactance of the line
R_{LINE}		= line resistance

As an illustration, we can use the phasor diagrams shown in Figs. 11(b) and 11(c). For the case of simplicity in the phasor diagram illustrations, we can simplify the equivalent circuit shown in Fig. 11(a) as an ideal transformer with only its leakage reactance represented. In Fig. 11(a), the real power P and reactive power Q are considered to be flowing from the right to the left

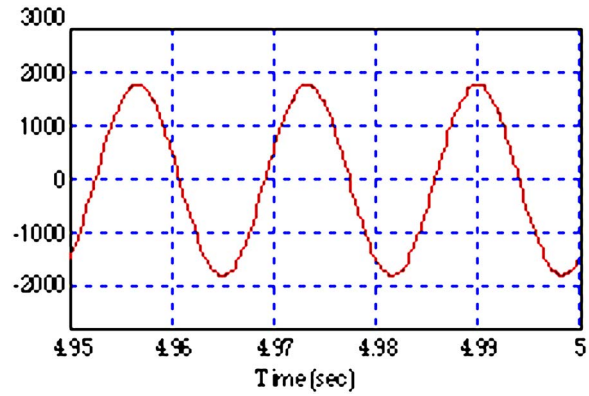


Fig. 13 Output current of a transformer under loaded condition

(positive values flow from the turbine to the grid). When $P > 0, Q < 0$ (the turbine generates real power but absorbs reactive power), then $E'_M < V_s$, and we have normal operation. On the other hand, when $P > 0, Q > 0$ (the turbine generates both real and reactive power), then $E'_M > V_s$ and we may experience saturation.

The resulting output current for operation under saturation is a distorted current waveform as shown in Fig. 12. The distorted portion of the current occurs because the transformer enters the nonlinear saturation region.

On the other hand, if the voltage drops across the leakage reactance and the winding resistance keep the voltage across the magnetizing branch from becoming excessively high, and the operation of the transformer remains in the linear region, the resulting output current is sinusoidal, as shown in Fig. 13.

One device that can mitigate transformer saturation is the tap changer—a device that enables real-time changes to the number of turns in the transformer winding. The purpose of the tap changer is to control the voltage on the output side of the transformer to be as constant as possible. For a given flux level, the magnetizing inductance L'_M will increase proportional to the square of the number of transformer turns, so for a given excitation voltage E'_M , with more turns we will get less magnetizing current I'_M and the transformer will operate in a less saturated condition (closer to the linear region). In essence, we can avoid the nonlinear saturation region completely if we have enough flexibility in the number of transformer turns that can be accessed with the tap changer.

5 Conclusion

This paper examines the nature of self-excitation and current harmonics generated by the fixed-speed induction generators commonly used in wind turbines. With proper design and control, based on detailed understanding of the wind/turbine transformer circuit dynamics, self-excitation and current harmonics can be controlled and/or eliminated.

Self-excitation can create concern about the safety of personnel repairing the line, but it can also be used to implement dynamic braking to control the speed of the turbine in a grid-loss situation and for other applications. Appropriately sized dynamic resistors and capacitors must be installed to ensure the desired operation characteristics.

Saturation of the magnetic circuit in the transformer and a resonance circuit between the capacitor compensation and the other circuit components can make the power system susceptible to harmonic distortions of the output current. The frequencies at which these distortions occur vary with wind speed because the reactive power of the wind turbine varies with wind speed. The power

factor, the power output of the wind turbine, and the potential use of a tap changer affect the level of transformer saturation and, thus, the nature of the harmonic distortion.

Acknowledgments

We acknowledge the support of the U.S. Department of Energy and we also thank Jorge Chacon from Southern California Edison for his help and discussions.

References

- [1] Sallan, J., Muljadi, E., Sanz, M., and Butterfield, C. P., 1999, "Control of Self-Excited Induction Generators Driven by Wind Turbines," Proc. 8th European Conference on Power Electronics and Applications Conference, EPE99, Lausanne, Switzerland, pp. 1–9.
- [2] Tang, L., Zavadil, R. M., Smith, J. C., and Childs, S., 1991, "Parametric Study of the Performance of a Passive Dynamic Brake," Proc. Windpower '91, Palm Spring, CA, AWEA, pp. 273–280.
- [3] Krause, P. C., 1986, *Analysis of Electric Machinery*, McGraw Hill Book Company, New York.
- [4] Neves, W., and Dommel, H., 1995, "Saturation Curve of Delta-Connected Transformer From Measurements," IEEE Trans. Power Deliv., **10**(3), pp. 1432–1437.
- [5] Dewan, S. B., Slemon, G. R., and Straughen, A., 1984, *Power Semiconductor Drives*, John Wiley and Sons, New York.
- [6] Fisher, M., 1991, *Power Electronics*, PWS Kent Publishing Company, Boston, MA.
- [7] VisSim/Simulink Translator User's Guide-Version 5, 2002, Visual Solutions, Inc.